600472

600472

DDC
RECEIVED
MAR 2 - 1964
TISIA F

63-1-6.60

6-74-64-19

A SEMI-THEORETICAL MODEL FOR ATMOSPHERIC PROPERTIES FROM 90 to 10,000 KM

Albert D. Anderson
William E. Francis

Work Performed under Lockheed Independent Research and
Defense Atomic Support Agency
Contract No. DA 49-146-XZ-204

May 1964

Research Laboratories
LOCKHEED MISSILES AND SPACE COMPANY

ABSTRACT

A semi-theoretical model of the upper atmosphere ~~has been~~ was constructed to allow the calculation of the primary atmospheric properties from 90 to 10,000 km altitude as a function of local time and solar activity. The calculations are based upon an empirical density profile from a density model as the initial input. Assuming diffusive equilibrium above 110 km and isothermal conditions above 400 km, the remaining properties (pressure, temperature, mean molecular mass, and the individual particle concentrations) are derived by using the hydrostatic equation and equation of state, together with boundary values from measurements.

To illustrate the model, two tables are given that present the average atmospheric properties vs altitude for sunspot maximum and minimum conditions, respectively, for the months immediately following the Argus (September 1958) and Starfish (July and August 1962) high-altitude nuclear detonations. ( )

A SEMI-THEORETICAL MODEL FOR ATMOSPHERIC PROPERTIES

FROM 90 to 10,000 KM

I. Introduction

The main geophysical problem connected with atmospheric structure in the heterosphere (Table 1) is to calculate accurate values for all the primary properties as a function of time, location, and date by taking into account the relevant processes. The primary atmospheric properties are temperature, density, pressure, and mean molecular mass (or composition). To account for their variations, the following factors must be considered: (a) time (hour, day, sun-rotation period, season, year, sunspot cycle); (b) location (altitude, latitude, longitude); (c) solar activity (ultraviolet radiation, X-rays, solar plasma and associated magnetic storms); and (d) processes (conduction, diffusion, mass transport, photoionization, dissociation, recombination, particle escape into space). The problem of describing atmospheric behavior is difficult because many of the above elements are interrelated.

Theoretical attempts have been made to form a model of the high atmosphere, that is, explain the observed properties in terms of the processes of photoionization and recombination. However, these fundamental attempts have been vitiated by ignorance of the solar ionizing spectrum and uncertainties in the absorption and ionizing cross sections and rate coefficients for the various possible ionic reactions. For example, the

rate coefficients for many upper atmosphere reactions are not known by direct measurement but are inferred from certain laboratory experiments conducted at various equilibrium conditions. Consequently, the uncertainty in the rate coefficients extends over several orders of magnitude. For these reasons, present data and theory regarding reactions between incoming solar radiation and atoms and molecules in the upper atmosphere are not sufficient to provide a basis for accurate calculations of atmospheric properties.

The magnitudes of various atmospheric properties in the heterosphere can be derived from measurements made from satellites, rockets, meteor observations, sky emissions, and the propagation of sound and radio waves. Although the frequency and accuracy of the various measurements are increasing, the data still are few and contain much uncertainty. The density (drag) data resulting from tracking satellites are generally considered the most precise and are by far the most numerous. However, the sparseness of the data in time and space requires the aid of a model to represent the variations of the atmospheric conditions in a continuous fashion. Therefore, greater understanding of the upper atmosphere has been attempted through an accurate description of all phases of its complex processes by means of models.

A. A New Atmospheric Property Model. The approach followed in the construction of most models is to assume the altitude dependence of some properties in order to calculate those remaining. Most of the models deal principally with density, pressure and/or temperature. The altitude variation of the mean molecular mass is often introduced somewhat arbitrarily,

and therefore, a physically consistent vertical distribution of the composition cannot be obtained. None of these models has been too successful in gaining wide acceptance.

To avoid some of the assumptions of other methods and to take into account some factors previously neglected, a new method has been devised for computing atmospheric properties. In this work, no major assumptions are made regarding the property profiles. Instead, the primary properties are calculated by starting with an empirical density profile derived from a density model as the primary input, assuming diffusive equilibrium above 110 km and isothermal conditions with altitude above 400 km. The density profile is represented by a previous empirical model (Anderson, 1964) as a function of local time and solar activity from 200 to 800 km. This density model uses corrected values of the 10.7-cm solar flux (called S ') as an index of the sun's extreme ultraviolet radiation in order to account for the marked variations in density that occur from day to day. The remaining properties are derived by using the hydrostatic equation and equation of state, to relate density, pressure, temperature, and mean molecular mass to altitude, together with boundary values based on measurements.

In summary, to develop a comprehensive model applicable from 90 to 10,000 km the theoretical and empirical approaches have been combined in such a way as to take advantage of the strong points of each by maximizing the number of constraints on the atmospheric properties and minimizing the number of assumptions. Since the calculations are quite tedious, this type of approach is feasible only with the use of modern computer

techniques. The model presented in this report has been programmed for an IBM-7090 computer.

II. Composition of the Upper Atmosphere

The main regions of the earth's atmosphere are presented in Table 1.

TABLE 1. The Main Regions of the Earth's Atmosphere

Atmospheric Region	Dominant Process	Sub Region	Altitude Range (km)	Remarks
Homosphere	Mixing	Troposphere	0 - 12	Mean molecular weight is constant
		Stratosphere	12 - 50	
		Mesosphere	50 - 90	
Heterosphere	Diffusion	Thermosphere	90 - 550	Frequent particle collisions
		Exosphere	550 - 60,000	Collisions rare; temperature constant to about 8500 km

Since the dominant process which controls atmospheric composition up to at least 90 km is mixing, the composition of the air remains the same up to this altitude. Hence, the mean molecular weight (mass) remains constant up to 90 km. (Above this height, the molecular weight decreases as the composition changes with altitude, because of molecular dissociation and diffusion.) Hence, the lower altitude boundary for the model was selected at 90 km. Below this altitude the U.S. Standard Atmosphere (1962) is perhaps the best available reference for atmospheric properties. A mean molecular weight of 28.96 is taken from this reference at 90 km. This value is calculated from the composition of dry air as given in Table 2.

TABLE 2. Normal Composition of Clean, Dry Atmospheric Air Near Sea Level From U. S. Standard Atmosphere, 1962

Constituent Gas	Content (Per Cent by Volume)	Molecular Weight
Molecular Nitrogen	78.084	28.0134
Molecular Oxygen	20.9476	31.9988
Argon	0.934	39.948
Carbon Dioxide	0.0314	44.00995
Neon	0.001818	20.183
Helium	0.000524	4.026
Krypton	0.000114	83.80
Xenon	0.0000087	131.30
Molecular Hydrogen	0.00005	2.01594
Methane	0.0002	16.04303
Nitrous Oxide	0.00005	44.0128

Seasonal and latitudinal variations at 90 km can be taken into account, if desired, by using values from the supplemental atmospheres derived by Court et al (1962). Table 3 gives temperature and density values for the U. S. Standard Atmosphere, 1962, and the supplemental atmospheres at 15°N, 30°N, and 45°N. The Tropical atmosphere represents mean annual conditions at 15°N, a region with little seasonal variability; the Sub-tropical and Mid-latitude atmospheres depict mean winter and summer conditions at 30°N and 45°N, respectively. Since the U. S. Standard Atmosphere, 1962, is a

middle-latitude (approximate 45°) year-round mean over the range of solar activity between sunspot minima and maxima, the summer and winter temperature and density values given for the Mid-latitude (45°N atmosphere in Table 3 can be used to estimate the seasonal variability at 90 km in the northern hemisphere. However, for the model given in this report, no seasonal or latitudinal variability is taken into account at 90 km. Therefore, a temperature of 181°K and a density of 3.17×10^{-9} gm cm^{-3} are taken to apply at 90 km.

TABLE 3. Atmospheric Temperatures and Density at 90 km

Standard Atmosphere	Temperature (K)			Density (gm/cm^3)		
	Summer	Winter	Average	Summer	Winter	Average
U.S. Standard 1962	-	-	181	-	-	3.17×10^{-9}
Mid-latitude (45°N)	174	204	-	3.60×10^{-9}	3.32×10^{-9}	-
Sub-tropical (30°N)	179	191	-	3.37×10^{-9}	3.45×10^{-9}	-
Tropical	-	-	184	-	-	3.52×10^{-9}

The composition of the upper atmosphere can be explained, at least in a qualitative sense, by noting the types of photochemical reactions that can occur. In the following paragraphs, the reactions leading to the neutral constituents will be discussed first, followed by the ion reactions.

A. Oxygen Dissociation and Recombination. At about 100 km, the absorption of solar radiation with wavelengths shorter than 1850 A down to about 1300 A leads to the dissociation of oxygen molecules, thus

$$O_2 + h\upsilon \rightarrow O + O \ . \tag{1}$$

For wavelengths shorter than 1026 A, the oxygen molecule can be ionized,

$$O_2 + h\upsilon \rightarrow O_2^+ + e \ . \tag{2}$$

This ionization is normally followed by a dissociative recombination,

$$O_2^+ + e \rightarrow O + O \ . \tag{3}$$

Although the oxygen atoms can recombine into molecules, photochemical equilibrium, where the rates of dissociation and recombination are equal at each altitude, does not prevail. Instead vertical transport due to both diffusion and mixing plays an important role in determining the atomic and molecular concentrations at various levels near 100 km. Nicolet (1959) has pointed out that the occurrence of oxygen dissociation in a region where diffusive transport is important makes it impossible to deduce either the degree of dissociation or the relative concentration of atomic oxygen and molecular nitrogen from measurements of molecular oxygen and atmospheric density. More oxygen dissociates than recombines above 100 km, due to the rapid fall off with altitude of the recombination processes. Below 100 km collisions occur frequently enough for recombination to prevail, hence more oxygen recombines than dissociates. Consequently, there is a steady flux of molecular oxygen upward and atomic oxygen downward through the 100 km level, due to the effects of diffusion and mixing. Extreme ultraviolet

monochromator measurements by Hinteregger (1962) show that atomic oxygen becomes the dominant atmospheric constituent above approximately 150 km altitude.

B. Nitrogen Dissociation and Recombination. The most active process leading to the dissociation of molecular nitrogen is ionization followed by dissociative recombination,

$$N_2^+ + e \rightarrow N + N \ . \tag{4}$$

Atomic nitrogen can react with molecular oxygen to form nitrous oxide and atomic oxygen,

$$N + O_2 \rightarrow NO + O \ . \tag{5}$$

The nitrous oxide in turn reacts with atomic nitrogen to form molecular nitrogen and atomic oxygen,

$$N + NO \rightarrow N_2 + O \ . \tag{6}$$

The effectiveness of these reactions, together with the slowness with which molecular nitrogen dissociates, causes atmospheric nitrogen to remain predominantly in molecular form. The monochromator measurements by Hinteregger (1962) indicate that atomic nitrogen is a minor atmospheric constituent below 225-km altitude.

C. Atomic Hydrogen. Photodissociation of water vapor and methane near 80 km constitute the principal sources of atomic hydrogen. Thus, for water vapor,

$$H_2O + h\upsilon \rightarrow H + OH \ . \tag{7}$$

This reaction is usually followed by,

$$OH + O \rightarrow H + O_2 . \qquad (8)$$

Owing to the small mass of the hydrogen atom compared to other atmospheric constituents, the hydrogen concentration does not decrease with altitude as rapidly as do the other atmospheric constituents in the altitude region where diffusion proceeds rapidly; hence atomic hydrogen becomes an increasingly important atmospheric constituent with increasing altitude. Atomic hydrogen, a minor constituent in the thermosphere, becomes the dominant constituent above 1500 to 2500 km altitude, and remains dominant up to 20,000 km where the hydrogen ion becomes dominant.

The distribution of atomic hydrogen out to 60,000 km from the earth at the extremes of the sunspot cycle, according to Johnson (1961a) is shown in Fig. 1. Two curves are shown, one for the maximum of the sunspot cycle (average temperature of 1500 K) and one for the minimum (average temperature of 1000 K). The source of atomic hydrogen near 80 km can be expected to remain essentially constant through the sunspot cycle, but the rate of escape, depending on the temperature at the base of the exosphere varies with the sunspot cycle. The escape will be relatively rapid when the temperature is high, and the concentration of hydrogen will be correspondingly low in the exosphere near sunspot maximum. The escape is relatively slow when the temperature is low, so that the concentration must be comparatively high near sunspot minimum.

D. Helium. Nicolet (1961) showed that helium atoms are an important constituent in the lower exosphere. He explains the high densities derived from the rate of change of the period of Echo satellite by the presence of

helium. Evidently, atomic oxygen, nitrogen or hydrogen cannot explain the slow density decrease between 750 and 1500 km. Although atomic oxygen is the most important constituent in the upper thermosphere, atomic helium dominates over atomic oxygen somewhere above 800 to 1000 km. Atomic hydrogen dominates over helium somewhere above 1500 to 2500 km.

E. Ionospheric Composition. The primary ions formed in the E region (85 to 140 km) of the ionosphere are N_2^+, O_2^+, and O^+. The N_2^+ ions dissociatively combine very rapidly, and they may also react with oxygen, so that the concentration of N_2^+ is small. Ion-atom exchange reactions of the type

$$X^+ + YZ = XY^+ + Z \tag{9}$$

proceed very rapidly, so that the reactions of O^+ with O_2 and N_2 quickly remove the O^+ ions and produce either NO^+ or O_2^+. The dominant ions in the F_1 region (140 to 200 km) are NO^+ and O_2^+ near the lower altitude boundary, with a gradual transition to O^+ as the principal ion at the upper boundary. O^+ becomes the dominant ion because of the rapid decrease with altitude of the neutral molecular constituents that otherwise would tend to eliminate O^+ by reaction (9). In the F_2 region (200 to 800 km), the ions present are O^+ and N^+, with O^+ greatly predominant. The helium ion starts to become dominant between 800 and 1400 km (Bourdeau and Bauer, 1963), depending on atmospheric temperature. Likewise, protons become the dominant ion between about 1400 to 4000 km. Thus, there are two transition regions (from oxygen to helium ions and from helium to hydrogen ions) in the upper ionosphere rather than a single transition from oxygen to hydrogen

as previously believed. The outer portion of the earth's atmosphere (extending from about 20,000 km to at least 40,000 km above the earth's surface) consists mainly of protons. The protons predominate in the earth's outer atmosphere over the hydrogen atoms because the confining effect of the earth's magnetic field makes their rate of escape to space much less than for the neutral hydrogen atoms.

III. The Physics of the Upper Atmosphere

Assuming that the earth's atmosphere is a continuous medium consisting of a gas in static equilibrium, the equation connecting the pressure P and density ρ at any altitude h is

$$dP = -g \rho \, dh , \tag{10}$$

where g is the gravitational acceleration. The variation in g with altitude can be taken into account by using the relationship

$$g = g_o R_o^2/(R_o + h)^2, \tag{11}$$

where g_o is the acceleration of gravity at the earth's surface and R_o is the earth's radius. Eq. 10 is the hydrostatic equation in differential form. Further, let m be the mean molecular mass of the gas and n denote the number density or concentration; the density ρ is then

$$\rho = n m . \tag{12}$$

Since the terrestrial atmosphere is almost a perfect gas, the pressure is given by the equation of state

$$P = n k T , \tag{13}$$

where T is the temperature and k the Boltzmann constant (1.38×10^{-16} erg deg^{-1}).

Multiplying both sides of (12) by g and dividing the result into (13), gives

$$P/\rho\, g = kT/mg = H, \tag{14}$$

where $H = kT/mg$ is known as the pressure scale height, a parameter convenient for atmospheric calculations. It should not be confused with the density scale height, $-\rho/(d\rho/dh)$, a parameter used to relate density to satellite drag (Anderson, 1964).

Above 400 km ions are distributed independent of the neutral particles as a result of diffusive equilibrium. The scale height H_i of a plasma (an electrically-neutral combination of ions and electrons) containing a single ionic species of mass m_i and temperature T_i is, neglecting the mass of the electron with respect to the ions, from (14),

$$H_i = k\,(T_i + T_e)/\, m_i g\ , \tag{15}$$

where T_e is the temperature of the electrons.

Even though immediately after formation the ions may have more than thermal energy, they speedily lose the excess by colliding with neutral particles, so that their temperature becomes the same as that of the neutral particles. This may not be true for the electrons because of the large mass difference. However, if the ions and electrons are in thermal equilibrium, $T_e = T_i = T$ in (15) and the ions and neutrals have the same mass, the scale height for the ions and electrons is then

$$H_i = 2\ kT/mg\ . \tag{16}$$

Thus, the ion scale height is twice that for neutral particles of the same mass. The electric field established between the electrons and ions just cancels half the gravitational force acting on the ions. When there are several kinds of ions, the average electric field is determined by the mean ionic mass $\bar{m}$. For an ion of mass m, the effect of the electrostatic field required to maintain charge neutrality is equivalent to changing gravity by the factor $(1 - \bar{m}/2m)$. All ionic constituents will be subjected to the same average electric field. Mange (1960) gives a method for calculating the altitude distribution of ionic constituents in electrostatic equilibrium.

Eq. 10 to 16 are applicable in the atmosphere where: (a) the escape into space of a constituent is not important, (b) the earth's magnetic field does not change the vertical distribution, and (c) the effect of the earth's axial rotation is negligible. Each of the above factors will now be considered in turn.

A. Accuracy of the Hydrostatic Assumption. The hydrostatic equation (10) is based on the concept of local thermodynamic equilibrium in which collisions between particles are frequent enough so that there is a complete statistical exchange of particle energy and momentum in the volume under consideration. In the thermosphere the particles collide often enough to insure a Maxwellian velocity distribution and the existence of a meaningful kinetic temperature. In the exosphere, above about 500 km, collisions are sufficiently reduced so that the existence of a Maxwellian distribution, and consequently, the validity of applying the hydrostatic relationship, must be examined anew. Liouville's theorem can be used to show that the Maxwellian velocity

distribution present below the base of the exosphere applies equally well in the exosphere, provided that the escape of particles to space is negligible (Herring and Kyle, 1961). The atmosphere is so rarefied in the exosphere that there is very little solar radiation absorbed. Also, there are no energy loss mechanisms to disturb the Maxwellian velocity distribution (Sharp, 1962). If the neutral particles have a Maxwellian velocity distribution, the ion velocities must also have the same distribution and a meaningful kinetic temperature. Thus, if the ion and neutral particle temperatures are the same in the thermosphere, they must also be the same in the exosphere wherever the neutral particles have a Maxwellian velocity distribution. At the temperatures present, the distribution is disturbed only by the escape of hydrogen from well above the base of the exosphere. Since at very high altitudes, (a) the hydrogen ion density is comparable to or higher than the neutral hydrogen density, and (b) the collision cross section for the ions is much larger than that for the neutral particles, it follows that the maximum altitude in the atmosphere where the hydrostatic equation is applicable can be determined by calculating the altitude in the exosphere where the density of the neutral hydrogen starts to be significantly affected by the escape of hydrogen atoms.

Johnson (1961b) divides the Maxwellian velocity distribution of exospheric particles into four groups depending on their trajectories with reference to the base of the exosphere. These four groups are: (1) particles with less than escape velocity that have come up to the level concerned on elliptic paths from the base of the exosphere; (2) particles with less than escape velocity whose perigees lie entirely above the base of the exosphere (these particles are in trapped orbits); (3) particles with more than escape

velocity whose perigees lie below the base of the exosphere (half of these particles, designated group 3a, are in the process of escaping, having attained escape velocity in a collision near the base of the exosphere; the remaining half, designated group 3b, are in the process of being captured from space); (4) particles with more than escape velocity whose perigees lie above the base of the exosphere (these are particles from space that approach the earth less closely than the base of the exosphere). The corresponding normalized groups are designated x_1, x_2, x_3, and x_4, respectively. One of us has expressed these fractional groups in terms of error functions in Appendix A of this report. These analytical expressions for the above distributions (Eq. 1, 2, 3, and 4 in Appendix A) can be used to calculate exospheric densities out to about 5 earth radii. Fig. 2 presents curves derived from the results of calculations made for the fraction of particles present in a Maxwellian distribution and also present in the atmosphere as a function of altitude h above the earth's surface, out to 10,000 km for three selected temperatures, 875K, 1125K, and 1625K. The curves start at h = 400 km since, for reasons given later, the atmospheric temperature above 400 km over a given location on the earth's surface does not vary with altitude. Consequently, for a given solar activity, the curves could be labeled also according to local times instead of temperatures. The temperature of 875K corresponds approximately to a nighttime temperature near sunspot minimum conditions, while the temperature of 1625K is a day time temperature during sunspot maximum conditions (Anderson, 1964). The 1125K temperature represents a 24-hr. mean for average solar activity conditions.

Two sets of curves are shown in Fig. 2 for the two cases: (a) $1-x_4$, $-x_3/2$, since in the actual distribution groups 3b and 4 are clearly absent, as the hydrogen concentrations in interplanetary space are too small to contribute significantly to the hydrogen captured by the earth and (b) $1-x_4 -x_3/2 -x_2$, with particles in group 2 absent. With regard to group 2 particles, Brandt and Chamberlain (1960) argue that they are present (case a), while Opik and Singer (1960) argue that they are not (case b). Since the results of the calculations made for the two cases are markedly different, both cases have been shown in Fig. 2 for comparison. If it is assumed that the hydrostatic equation can no longer be used to make accurate calculations for those conditions in which the fraction of Maxwellian particles is below 0.90, then for an average temperature of 1125K it can be applied accurately out to 8500 km if case (a) holds or only out to 2900 km if case (b) holds. However, Johnson (1961b) has considered both cases and suggests it is likely that the trapped orbits are populated out to 6 or 7 earth radii. Since some collisions occur above the base of the exosphere, there will be some injection of particles into trapped orbits in the lower exosphere. Also, the presence of ionized hydrogen with a Maxwellian velocity distribution out to 5 or 6 earth radii (Johnson, 1960b) contributes to the population of trapped orbits for neutral particles; charge exchange can occur between the neutral hydrogen (principally group 1 particles) and the ionized hydrogen, tending to fill the trapped orbits. Therefore, following Johnson, the constraints imposed by case (a), rather than case (b), were adopted for the model. Fig. 2 indicates that the error involved for either case will increase with altitude and temperature. The greatest error in using the

hydrostatic assumption will occur, as illustrated in Fig.2, during the day near sunspot maximum conditions. For case (a) the error will start to become significant above about 5000 km above the earth's surface.

B. Effect of the Earth's Magnetic Field on the Vertical Distribution of Particles. The magnetic field affects the distribution of ions, but not the distribution of neutral particles. Since the mean free path for the protons and electrons are long compared with the cyclotron radii, the average motion of the protons and electrons is along the magnetic field lines, and the mean motion of the particles is not isotropic. However, Johnson (1960b) points out that the detailed velocity distribution remains isotropic, even if the mean motion of the particles is not, if collisions among the protons and electrons remain rather frequent. Out to 10,000 km, at least, collisions do remain frequent enough, on the order of one per second, even for particle concentrations and night time temperatures present near solar minimum. The distribution of ions must follow the hydrostatic relationship so long as the detailed velocity distribution remains isotropic (Spitzer, 1952).

C. Effects of the Earth's Axial Rotation on Ion Distribution. The magnetic field affects the distribution of ions by linking the ion-electron plasma in the exosphere to the lower ionosphere, thus requiring that the plasma rotate with the earth. The resulting centrifugal force on the ions modifies the gravitational attraction that enters into the hydrostatic equation. Since all the ions and electrons, wherever they may be in the magnetic field, must rotate with the earth, the generalized hydrostatic equation must be corrected for the earth's rotation. The modified hydrostatic equation

for the distribution of ions or electrons in a region where diffusive equilibrium prevails is (Johnson, 1960b)

$$N(h) = N_o \exp [g_o R_o^2 m/(R_o+h)\ 2kT] . \exp [m\ \Omega^2 (R_o+h)^2 \cos^2\theta/4kT], \quad (17)$$

where N(h) is the number density at altitude h, N_o is a normalization constant, g_o is the acceleration of gravity at the earth's surface, R_o is the radius of the earth, m is the ion mass, Ω is the rotational velocity of the earth about its axis, θ is the geocentric angle between the equatorial plane and the point considered (i.e. latitude), and k the Boltzmann constant. The first exponential is the normal relationship, and the second exponential represents the modification due to the centrifugal force (At h = 10,000 km, the maximum value of the second exponential occurs over the earth's equator and is inversely proportional to the temperature. For T = 800K, it is 1.05).

D. Diffusive Equilibrium. Inasmuch as the atmosphere consists of a mixture of gases subject to a force field, the equilibrium distribution of its constituents can be expected to show some degree of diffusive separation. Although turbulent mixing below 100 km does not allow the development of diffusive equilibrium distributions, above this altitude there is experimental evidence that diffusive separation commences. In the geopotential field, diffusive equilibrium gives a concentration distribution for each neutral species that varies exponentially with the geopotential, with a more rapid decrease in concentration with increasing geopotential for the heavier constituents in the atmosphere than for the lighter (Chapman, 1960). The result is a static distribution of gas constituents under the action of the external force field, expressed by the hydrostatic relationship applying

for each atmospheric constituent independently of the others. This generalization holds for the isothermal conditions that always exist above 400 km. Below this altitude, the temperature gradient present introduces the effect of thermal diffusion, which slightly modifies the conclusion.

From (10), (12), and (13),

$$dP_1 = -\rho_1 \, g \, dh = -n_1 \, m_1 \, g \, dh = \frac{-P_1}{kT} m_1 \, g \, dh \, , \qquad (18)$$

where the subscript 1 refers to a particular neutral constituent having density ρ_1, concentration n_1, molecular mass m_1, and partial pressure P_1. Likewise, for another constituent whose concentration is n_2, molecular mass m_2, and partial pressure P_2.

$$\frac{dP_2}{m_2 P_2} = -\frac{g \, dh}{kT} \qquad (19)$$

If both constituents are at the same altitude h, then

$$\frac{dP_2}{m_2 P_2} = \frac{dP_1}{m_1 P_1} \qquad (20)$$

Integrating both sides of (20), the left side from pressure $P_2(h_1)$ to pressure $P_2(h_2)$, corresponding to altitude h_1 and h_2, respectively, and the right side from $P_1(h_1)$ to $P_1(h_2)$, gives

$$\int_{P_2(h_1)}^{P_2(h_2)} \frac{dP_2}{P_2} = \frac{m_2}{m_1} \int_{P_1(h_1)}^{P_1(h_2)} \frac{dP_1}{P_1} \qquad \text{or}$$

$$\frac{P_2(h_2)}{P_2(h_1)} = \left[\frac{P_1(h_2)}{P_1(h_1)}\right]^{\frac{m_2}{m_1}} . \tag{21}$$

Thus, if the pressure altitude dependence of one neutral constituent is known, the others can be determined by (21). If j is the total number of constituents, it follows from Dalton's law that

$$\sum_{i=1}^{j} P_i(h_1) = P(h_1) , \tag{22}$$

and

$$\sum_{i=1}^{j} P_i(h_2) = P(h_2) , \tag{23}$$

where $P(h_1)$ and $P(h_2)$ are the total pressures at altitudes h_1 and h_2, respectively. If the partial pressures are known for each of the j constituents at one pressure altitude $P(h_1)$, they can be determined for any other pressure altitude $P(h_2)$ from (21) and (23) provided that diffusive equilibrium exists from h_1 to h_2.

With regard to ions, Johnson (1960b) points out that above the F_2 maximum in the ionosphere (300-350 km), diffusion becomes so rapid that it, rather than recombination becomes the dominant factor controlling the ion distribution. Diffusion of ions through the neutral gas tends to distribute the ions so that they satisfy a hydrostatic law (see paragraph following Eq. 16) independently of the neutral particles.

During 1956-1958 the Naval Research Laboratory launched four rockets instrumented with radio-frequency mass spectrometers to study neutral gas composition above 100 km at Churchill, Canada (59°N). Results from the flights, two at night and two during the day, showed that diffusive separation started in the approximate range from 100 to 120 km (Meadows and Townsend, 1960). USSR measurements made during the night in September 1960 indicated that the height of the beginning of diffusion was about 110 km (Pokhunkov, 1962). In view of the foregoing, the altitude where diffusive equilibrium begins is tentatively taken at 110 km for the model in this report. This altitude may be changed later when more knowledge becomes available concerning diurnal, latitude, seasonal, and solar effects on the exact altitude where diffusive separation starts.

E. Isothermal Conditions. The concept that the atmosphere extending above 400 km over a given location on the earth's surface is isothermal in the sense that the temperature does not vary with altitude is now well established. In the tenuous gas of the upper thermosphere the thermal conductivity is independent of the pressure while the heat capacity varies linearly with density. Consequently, the conductivity is very large compared to the heat capacity (Johnson, 1956). Above 400 km, the absorption of energy is negligible and the relatively high heat conductivity eliminates temperature differences; hence the temperature is nearly constant with altitude for many thousands of kilometers. Nicolet (1960) has concluded that the time of conduction is so short that there is a strong tendency to a vertical isothermy for the atmosphere at high altitudes above a given region of the earth.

Spitzer (1949) first pointed out that the outermost atmosphere or exosphere, the region in the atmosphere in which collisions are relatively rare, should be isothermal, that is, that the distribution of atoms in the exosphere should be that of an isothermal gas. The base of the exosphere is defined as the level at which the mean free path is equal to a scale height H (Eq. 14). Its altitude usually lies between 450 to 650 km. The upper extent of the exosphere may be taken to coincide with the outer edge of the magnetosphere, extending out to at least 40,000 km above the earth's surface (Beard, 1960).

The principal heat source in the upper atmosphere above 130 km is the extreme ultraviolet radiation (EUV) from the sun having wavelengths from 200 to 900 A. Magnetic (corpuscular) heating is not important under normal conditions, but during the disturbed conditions accompanying major magnetic storms, it can lead to transient heating increases. Fig. 3 (Friedman, 1959) shows the altitude at which a fraction 1/e remains of the radiation incident on the atmosphere. Almost all of the energy of the incident EUV radiation is absorbed by the main atmospheric constituents O_2, O and N_2 in the altitude region from 100 to 200 km. The radiation absorbed below 200 km is responsible for heating the atmosphere at altitudes extending many thousands of kilometers above 200 km (Johnson, 1958). The degree of heating (represented by the temperature of the isothermal atmosphere) is proportional to the energy absorbed in the region between 100 and 200 km. The amount of energy absorbed depends on its intensity near the top of the absorbing region, which is a function of (a) solar activity, and (b) the location of the absorbing region with respect to the sun-earth line. Hence, the portions of

the exosphere over different regions of the earth each will have different isothermal temperatures. Anderson (1964) takes (a) into account by using the parameter S' as an index of the EUV emitted from the sun; the effect of (b) is described by using t, the local time, as a parameter. These two parameters can be used also to represent the variation of the exospheric temperature in the night hemisphere, inasmuch as the nighttime temperature in a given region of the exosphere depends on the temperature existing before sunset in the corresponding lower absorbing region of the thermosphere (a function of S') and on the rate of cooling of this lower region with time after sunset (a function of t). An estimate of the temperature in the upper thermosphere and lower exosphere as a function of S' and t is shown in Fig. 4.

The altitude of the thermopause is subject to a considerable diurnal variation varying with the amount of EUV abosrbed between 100 and 200 km; it is a maximum in the sunlit atmosphere and a minimum in the dark atmosphere. During the day at sunspot maximum, the altitude of the thermopause is about 400 km; during the night at sunspot minimum, its altitude is about 200 km. Most of the solar energy absorbed below 200 km is conducted downward to below 120 km where it is dissipated by infrared radiation. Thus, there is a steep positive temperature gradient between 100 and 200 km ending at the thermopause or the level above which the atmosphere becomes isothermal. Above 120 km, the atmosphere is a very poor radiator in the infrared, but below 100 km, the atmosphere is a much better radiator because of the presence of H_2O, OH, CO_2 and O_3.

The isothermal temperature used in the model is the kinetic temperature that can be determined only for a gas with a Maxwellian velocity distribution. As pointed out under the discussion of the accuracy of the hydrostatic assumption, the Maxwellian velocity distribution applies in the exosphere provided that the escape of particles to space is negligible. For hydrogen, the escape of atoms is comparatively rapid so that the velocity distribution of hydrogen atoms in the upper exosphere is not Maxwellian. Therefore, the hydrogen atoms in the upper exosphere have a non-Maxwellian distribution that becomes more pronounced with altitude. Under these circumstances the concept of kinetic temperature is not entirely applicable, although an effective temperature can be defined by considering the average energy of the hydrogen atoms. This effective temperature is not constant as a function of distance from the earth. The same altitude above which the use of the hydrostatic equation becomes questionable in the model can also be taken to be where the deviation between the kinetic and effective temperature becomes significant. This altitude, above which the fraction of Maxwellian particles was below 0.90, was at 8500 km for an average temperature of 1125 K, assuming particles are present in trapped orbit. Sharp (1962, Fig. 5) indicates the effective temperature decreases with distance out to 10 earth radii for an assumed kinetic temperature of 1000 K at the base of the exosphere.

IV. The Empirical Density Model

In this section, the empirical density model used to derive the primary input for the atmospheric property model will be described in brief. It [illegible] [illegible]ented in detail elsewhere (Anderson, 1962, 1964). The density ρ, [illegible], is represented by

$$\rho = K'' S'^{N} , \qquad (24)$$

where K" and N are constants for a given altitude h and local time t, and S' is a daily index of the sun's extreme ultraviolet radiation expressed in units of 10^{-22} watt m^{-2} cps^{-1}. K" and N are presented in tables (Anderson, 1964) for selected altitudes from 200 to 800 km and every hour. Hence, using (24) together with the tables, the density and its variations can be readily calculated as a function of S', derived from the relative variations of the sun's 10.7-cm flux (S) and satellite drag data. Table 4 gives average values for S' and S by months, 1958 to 1962. Eq. 24 has been programmed for an IBM-7090 computer; the K" and N values corresponding to a given h (nearest kilometer) and t (nearest 4 minutes) are found from the tables by logrithmic interpolation for K" and linear interpolation for N. Since the results of previous work indicate that density variations with latitude are small, at least between 60 N and 60 S, they have been neglected in this model.

TABLE 4.

Average S' and S (10^{-22} watt m^{-2} cps^{-1}) by months, 1958 to 1962.

Month	1958		1959		1960		1961		1962	
	S'	S	S'	S	S'	S	S'	S	S'	S
January	-	-	245	271	199	200	110	120	55	93
February	254	210	252	206	181	169	94	105	62	101
March	279	250	256	228	174	146	110	104	73	100
April	322	246	241	210	189	167	92	105	81	96
May	272	219	209	213	147	163	81	99	62	98
June	208	220	184	217	133	162	75	110	55	91
July	212	224	180	203	130	164	78	116	42	81
August	224	237	187	234	153	174	78	106	46	77
September	272	243	207	194	169	164	82	112	65	89
October	286	226	189	164	163	141	79	96	70	87
November	249	207	209	183	160	147	69	89	65	84
December	265	234	189	179	134	136	65	93	56	81
All Months	258	228	212	208	161	161	84	104	61	90

V. The Model for Atmospheric Properties from 90 to 10,000 km

In this section the method used to derive a comprehensive model for atmospheric properties will be given in detail. This model, covering the altitude range from 90 to 10,000 km, originates from the attempt to apply the principles presented in the preceding sections together with observational data so as to minimize the number of assumptions needed and maximize the

accuracy of the calculations. Major reliances has been placed on using the density values from the density model in section 4 as primary input; starting with this, emphasis has been placed on developing a procedure to calculate the remaining properties. The physical laws that are assumed to apply are the hydrostatic equation and the equation of state. It is also assumed that diffusive separation occurs above 110 km and that isothermal conditions are present above 400 km.

A. Derivation of 500- to 200-km Pressure Profile from Density Profile. The first step involved in calculating the atmospheric properties is to derive a pressure profile from the input density profile (Eq. 24) for the 200 to 800 km altitude range and for a given S' and t. Kallmann (1959) has given a method for obtaining a pressure profile from a density profile in which both profiles have the same comparable accuracy, although the former covers a lesser altitude range. If (10) is integrated between two levels h_1 and h_2, where $h_2 > h_1$, the explicit relation for the pressure at h_1, $P(h_1)$, is

$$P(h_1) = P(h_2) + \int_{h_1}^{h_2} g(h)\rho(h)\, dh, \qquad (25)$$

where $P(h_2)$ is the pressure at h_2 and $g(h)$ is given by (11).

From (12) and (13),

$$P = \rho\, k\, T/m\ . \qquad (26)$$

Using (26) and ρ, T, and M values from Anderson (1964), values of P were calculated near minimum (S' = 70 units, t = 5 hr) and near maximum (S' = 200, t = 14 hr) sunspot conditions at both 800 km and 500 km. Table 5 presents these values, together with the ratio P_{800}/P_{500}, where P_{800} and P_{500}

are the pressures at 800 km and 500 km, respectively. If P_{800} is taken equal to zero, then the small magnitudes of the ratios in this table indicate that (25) can be used to calculate a fairly accurate pressure profile from about 500 to 200 km. The largest error in pressure (6 per cent) will occur at sunspot maximum at 500 km.

TABLE 5. Pressure Values near Sunspot Minimum ($S' = 70$, $t = 5$ hr) and near Sunspot Maximum ($S' = 200$, $t = 14$ hr)

Altitude (km)	Sunspot Minimum P (dynes/cm^2)	Sunspot Maximum P (dynes/cm^2)
800	1.21×10^{-8}	1.35×10^{-6}
500	7.03×10^{-7}	2.34×10^{-5}
	$\frac{P_{800}}{P_{500}} = .02$	$\frac{P_{800}}{P_{500}} = .06$

To evaluate the integral on the right side of (25), advantage was taken of the fact that, for functions whose behavior is approximately exponential, an accurate integration formula (Kallmann, 1959) is

$$\int_{h_1}^{h_2} F\,dh = \frac{F(h_2) - F(h_1)}{\ln F(h_2) - \ln F(h_1)} (h_2 - h_1) , \qquad (27)$$

where in this case $F = g(h)\ \rho(h)$ and $h_2 - h_1$ is taken to be a sufficiently small altitude increment. A step size of 5 km is used for the pressure calculation inasmuch as computations made in steps of 1 km were not significantly different.

B. Initial Conditions at 110 km. In this model the altitude where diffusive equilibrium begins is taken at 110 km, thus the initial property conditions must be specified at this altitude. If the constituent concentrations and temperature are specified for this altitude, the remaining atmospheric properties can be derived from them.

Schaefer and Nichols (1961, 1963), using a massenfilter, report values of 0.5 at 110 km for an O/O_2 ratio; these results are in general agreement with ultraviolet absorption results of Kupperian et al (1960), according to Schaefer (1963). However, they are at wide variance with previous rocket-borne mass spectrometer measurements. The major differences between Schaefer's and Nichols' experiment and those conducted in the past by other investigators were: (a) the analyzing instrument was a massenfilter instead of a Bennett mass spectrometer; (b) the instrumentation was ejected at altitude from within a volume pressurized with helium to minimize the effects of rocket-borne contaminants; and (c) the ion source was designed for direct immersion in the ambient atmosphere with the greatest possible open look angle to minimize the surface recombination of active constituents. The following values, based upon the results of Schaefer and Nichols (1963), were adopted for the constituent number densities at 110 km:

$$n(N_2) = 22.0 \times 10^{11}$$
$$n(O_2) = 5.0 \times 10^{11}$$
$$n(O) = 2.5 \times 10^{11}$$
$$n(A) = 0.16 \times 10^{11}$$

Hence, the total number density is $n = 2.97 \times 10^{12}$ particles cm^{-3}. The density is from (12),

$$\rho = \sum_{i=1}^{j} n_i m_i , \tag{28}$$

where m_i is the molecular mass for each of the j constituents. Using (28), the density at 110 km is $\rho = 1.36 \times 10^{-10}$ gm cm^{-3}, and the mean molecular mass is $m_{110} = \rho/n = 4.58 \times 10^{-23}$ gm.

The mean molecular weight M is

$$M = \frac{28.96\ m}{4.8 \times 10^{-23}} . \tag{29}$$

Hence, substituting m_{110} in (29), $M_{110} = 27.73$. The temperature at altitude h can be computed from the molecular-scale temperature $T_M(h)$ at the same altitude from

$$T_h = M_h\ T_M(h)/M_{90} , \tag{30}$$

where M_h and M_{90} are the mean molecular weights at h and 90 km altitude, respectively. Using the value $T_M(110) = 261$ K from the U. S. Standard Atmosphere (1962) in (30), $T_{110} = 250$ K. Finally, the partial pressure for each constituent P_i can be calculated at 110 km from (13), where

$$P_i = n_i\ k\ T . \tag{31}$$

The total pressure at 110 km computed from (13) is $P_{110} = 1.02 \times 10^{-1}$ dynes cm^{-2}.

These initial conditions for properties at 110 km will vary somewhat with solar activity and diurnally. Inasmuch as there is a lack of enough accurate measurements of these quentities at 110 km, their variations cannot be determined at present.

C. Atmospheric Properties from 90 to 100 km. Table 6 summarizes the above values of the atmospheric properties derived for 110 km; also presented are the values at 90 km from the U. S. Standard Atmosphere (1962) used in the model.

TABLE 6. Values of Atmospheric Properties at 90 and 110 km Used in Model

Altitude (km)	Density (gm cm^{-3})	Pressure (dynes cm^{-2})	Temperature (deg K)	Mean Molecular Weight	Number Density (cm^{-3})
90	3.17×10^{-9}	1.64	181	28.96	6.59×10^{13}
110	1.36×10^{-10}	1.02×10^{-1}	250	27.73	2.97×10^{12}

The mean molecular weight and temperature at any altitude h between 90 and 110 km can be computed by assuming a linear variation of these quantities. Hence,

$$T_h = T_{90} + \frac{(T_{110} - T_{90})}{20} (h - 90) \quad , \qquad (32)$$

and

$$M_h = M_{90} + \frac{(M_{110} - M_{90})}{20} (h - 90) \quad , \tag{33}$$

The pressure P_h at altitude h is calculated from (10) and (26), thus

$$dP = - \frac{P\, m\, g\, dh}{k\, T} \quad . \tag{34}$$

Dividing (34) by P and integrating from 90 to h km gives

$$\ln \frac{P_h}{P_{90}} = - \int_{90}^{h} \frac{mg\, dh}{k\, T} = - \frac{g_a}{R} \int_{90}^{h} \frac{M}{T}\, dh, \tag{35}$$

where g_a is the average acceleration of gravity between 90 and h km, and R is the universal gas constant, 8.317×10^7 erg mole^{-1} deg^{-1}. Hence, P_h can be found by substituting T_h from (32) and M_h from (33) in (35). Finally, the density at h can be derived from (26).

D. Atmospheric Properties from 110 to 500 km. Starting with the P_i at 110 km, given by (31), values can be computed for other altitudes up to 500 km by (21) and (23) (the total pressure P is not known accurately above 500 km). However, since P is known as a function of altitude h from 200 to 500 km, m (or M) can likewise be determined as a function of h for this same altitude interval. This follows from (28) and (31), where

$$m = \frac{1}{n} \sum_{i=1}^{j} n_i\, m_i = \frac{1}{P} \sum_{i=1}^{j} P_i\, m_i \quad . \tag{36}$$

Since ρ , m, and P are known as a function of h from 200 to 500 km, T can be calculated from (26). Practically, it is not necessary to calculate T above 400 km, since conditions are isothermal above this altitude. Finally, n_i can be calculated from (31).

However, P is not known as a function of h between 110 and 200 km. Its altitude variation in this altitude range is found by first deriving M as a function of altitude for this range. This is done by assuming the altitude variation of M to be as follows:

$$M = M_{110} + A\,(h - 110) + B\,(h - 110)^2 \,. \tag{37}$$

The polynomial (37) is a fairly accurate approximation because M decreases slowly from 110 to 200 km. Differentiating (37) with respect to h gives

$$\frac{dM}{dh} = A + 2B\,(h - 110) \tag{38}$$

At h = 110 km, B = 0, and $A = \left(\frac{dM}{dh}\right)_{110} \simeq \frac{M_{110} - M_{90}}{20}$.

At h = 200 km, $A + 180\,B = \left(\frac{dM}{dh}\right)_{200} \simeq \frac{M_{220} - M_{200}}{20}$, hence

$$B \simeq \frac{(M_{220} - M_{200}) - (M_{110} - M_{90})}{3600} \,.$$

P can be found as a function of h as follows: (a) starting with the known P_i at 110 km, solve (21) and (23) to find the P_i as a function of P from 110 km to 200 km; (b) the m value corresponding to P is found from (36); (c) then the corresponding altitude h is determined from (29) and (37).

To find ρ as a function of h from 110 to 200 km, it is assumed that P decreases exponentially with altitude between small altitude increments, thus

$$P_2 = P_1\, e^{-a_2\,(\phi_1 - \phi_2)} \,, \tag{39}$$

where P_1 and P_2 ($P_1 > P_2$) are the pressures at geopotential altitudes ϕ_1 and ϕ_2, respectively. The geopotential altitude ϕ is related to the geometric altitude h in meters as follows:

$$\phi = \frac{1}{9.80} \int_0^h g \, dh \, . \tag{40}$$

Therefore, ϕ_1 corresponds to h_1 and ϕ_2 corresponds to h_2. From (39),

$$a_2 = - \frac{\ln (P_2/P_1)}{\phi_1 - \phi_2} \, . \tag{41}$$

The density ρ_2 at geopotential altitude ϕ_2 is, from (10), (39), and (40),

$$\rho_2 = - \frac{dP_2}{d\phi} = -a_2 P_1 e^{-a_2 (\phi_1 - \phi_2)} = - a_2 P_2 \, . \tag{42}$$

Hence, (41) and (42) are used to calculate the density from 110 to 200 km. The remaining property, the temperature, can be calculated for this same altitude range from (26). The temperature value calculated at 200 km can be compared with that previously derived to provide a check on the accuracy of the computations.

E. Atmospheric Properties from 500 to 800 km. It was pointed out that the pressure profile derived from (25) was inaccurate from 800 to 500 km. The main difficulty was that the pressure at the starting altitude, 800 km, was not known. However, since the pressure at 500 km is known fairly accurately, (25) can be used to calculate the pressure upwards from 500 to 800 km. Also, since T and ρ are known from 500 to 800 km, m can be calculated from (26).

F. Neutral Particle Concentrations from 400 to 10,000 km. The neutral atmosphere above 400 km is comprised almost wholly of atomic oxygen, helium, and hydrogen; the relative concentrations of these constituents depend strongly on altitude and temperature. At a certain altitude h' between 500 and 800 km, depending on temperature, where atomic oxygen and helium comprise most of the atmosphere, the following equation (from eq. 23 and 31) holds:

$$P' - P_O \simeq P_{He} = n_{He}\, k\, T\ , \tag{43}$$

where P' is the total pressure previously calculated at h', and the subscripts O and He are for atomic oxygen and helium, respectively. Trial calculations indicate that h' $\simeq$ 600 km for S' < 100 units (T < 1100 K, Fig. 4) and h' $\simeq$ 700 km for S' > 100 units (T > 1100 K). To determine P_O at h' in (43), take (34) to apply for only one constituent of partial pressure P_i. Dividing (34) by P_i and integrating from h_1 to h_2, where $h_2 > h_1$, and using (11), gives

$$\ln \frac{P_i(h_2)}{P_i(h_1)} = -\frac{m_i}{k\,T} \int_{h_1}^{h_2} g\, dh = -\frac{m_i\, g_o\, R_o^2\, (h_1 - h_2)}{k\, T\left[R_o^2 + R_o(h_1 + h_2) + h_1 h_2\right]}\ . \tag{44}$$

Further, since the temperature and particle mass are constant with altitude,

$$\frac{P_i(h_2)}{P_i(h_1)} = \frac{n_i(h_2)}{n_i(h_1)} = \frac{\rho_i(h_2)}{\rho_i(h_1)}\ . \tag{45}$$

Hence, P_O is calculated from (44), where $P_i(h_1) = P_O(h')$ and $P_i(h_1) = P_O(500\ \text{km})$, and substituted in (43) to find P_{He} at h'. Using this base value, P_{He} and n_{He} were calculated from (44) and (45), respectively, from 400 to 10,000 km.

Also, using (44) and (45), P_O and n_O were calculated from 500 km out to an altitude, above about 2000 km, where atomic oxygen becomes negligible in concentration.

According to Fig. 1, the concentration of atomic hydrogen in the exosphere decreases with increasing temperature. If, as a first approximation, it is assumed that the concentration of atomic hydrogen n_H (atoms cm^{-3}) varies linearly with temperature T (deg Kelvin), then at 2000-km altitude from Fig. 1,

$$n_H = 5.1 \times 10^5 - 310\ T\ . \tag{46}$$

Using (44), (45), and (46), n_H can be calculated as a function of T from 400 to 10,000 km.

G. Ion Concentrations from 400 to 10,000 km. Although the total concentration of the neutral particles is at least an order of magnitude greater than that of the ions out to about 2000 km altitude, the ion concentrations finally become significant at the higher altitudes. The positively-charged part of the ionosphere above 400 km consists largely of oxygen, helium, and hydrogen in the singly-ionized state, with O^+ dominant up to about 800 km, He^+ dominant somewhere between 800 and 1400 km, and H^+ dominant somewhere above 1400 and 4000 km. Since this ionized gas must be electrically neutral, each unit volume contains equal numbers of negative charges (electrons) to match the positive charges. Therefore,

$$n_{ion} = n_e\ , \tag{47}$$

where n_{ion} and n_e are the numbers of ions and electrons in the same unit volume, respectively.

Bowles (1962) presents profiles of electron density over the magnetic equator obtained by the incoherent scattering technique from which n_e can be estimated as a function of temperature. Fig. 5 shows two electron concentration profiles plotted with geopotential altitude, labeled 1300 K and 800 K, derived from Bowles' data. Inasmuch as the positively charged part of the ionosphere above 1500 geopotential km consists almost wholly of H+, the temperatures corresponding to the curves in Fig. 5 can be calculated using Eq. 48, assuming thermal equilibrium prevails between H+ and the electrons. Thus,

$$T = \frac{m_{H^+} \; g_o \; R_o^2 \; (h_1 - h_2)}{2 \; k \; \ln \left[\frac{n_{H^+} \; (h_2)}{n_{H^+} \; (h_1)}\right] \left[R_o^2 + R_o \; (h_1 + h_2) + h_1 \; h_2 \right]} \tag{48}$$

The approximate T values of 1300 K and 800 K for the two curves were found from (48) by substituting in respective n_{H^+} (h_1) and n_{H^+} (h_2) values from both curves of Fig. 5, where $h_2 > h_1 > 1500$ geopotential km, and, from (47), n_{H^+} $(h_1) = n_e$ (h_1) and n_{H^+} $(h_2) = n_e$ (h_2).

To estimate n_{H^+} as a function of T, it is assumed that the concentration of H+ varies linearly with temperature T. Therefore, using concentration values from the curves of Fig. 5 at 5000 km altitude (2800 geopotential km from eq. 40),

$$n_{H^+} = 6.0 \times 10^2 + 8.00 \; (T - 800) \text{ at } h = 5000 \text{ km.} \tag{49}$$

Since the positive ions below 500 geopotential km are largely O+, the concentration of O+ as a function of T can be derived in the same manner as H+. Consequently,

$$n_{O^+} = 1.8 \times 10^5 + 920\ (T - 800) \text{ at } h = 550 \text{ km.} \qquad (50)$$

To find n_{He^+} as a function of T, concentration values were used from that altitude region of the atmosphere where the relative concentration of He+ was greatest. Accordingly, n_{He^+} values were determined from the two curves of Fig. 5 at 1000 km (865 geopotential km) by graphically subtracting extrapolated straight-line portions of the H+ and O+ curves. The equation for the linear variation of n_{He^+} with T is,

$$n_{He^+} = 4.0 \times 10^3 + 92.0\ (T - 800) \text{ at } h = 1000 \text{ km.} \qquad (51)$$

For a given S' and t, only one particular T value is used in (48) through (51). This is the temperature value at 400 km that can be taken also to apply at all higher altitudes up to about 8500 km. The height variation of an ionic constituent can be found by (48) in an altitude region where all other ionic constituents can be neglected. However, in regions from 400 to 10,000 km where no one ionic constituent is greatly predominant, the height variation of each constituent can be found from an equation given by Hanson (1962, equation 8a).

H. Atmospheric Properties from 8000 to 10,000 km. Because the n_i, corresponding to a given T, are known as a function of h from 800 to 10,000 km, P_i can be calculated from (31). Consequently, P can be found from (23). Then, m can be determined from (36), where n represents the sum of the neutral-particle and ion concentrations. Finally, ρ is computed from (26).

VI. Examples of Atmospheric Properties Calculated from Model for Sunspot Maximum and Minimum Conditions.

The equations in Section V are programed for an IBM-7090 computer. For the purpose of illustrating the model, two examples are given of computations; one example is selected to represent average conditions near sunspot maximum; the other example represents average conditions near sunspot minimum. The S' value used for the former (S' = 250) is an average value for September 1959, the month immediately following the Argus high-altitude nuclear detonation. The latter's S' value (S' = 44) is an average value for July and August 1962 (S' = 42 for July; S' = 46 for August), the two months following the Starfish high-altitude shot. Both examples are for t = 21 hr; the density for this time has been found to closely approximate the diurnally averaged density or the sum of the densities for every hour of the day divided by 24.

The results of the computations made from the model are given in two tables that present the atmospheric properties vs altitude from 100 to 10,000 km. Tables 7 and 8 exhibit the properties for S' = 250 units and S' = 44 units, respectively. In addition, the pressure scale height H(eq. 14), a commonly used parameter for upper-atmosphere calculations, is shown in column 6.

VII. Summary

It was pointed out in the introduction to this report that the approach followed by most models is to assume altitude profiles for some of the

TABLE 7. Upper Atmosphere Neutral Properties vs. Altitude Near Sunspot Maximum

Altitude	Temp.	Mol. Wt.	Density	Pressure	Scale Ht.	Total Conc.		Constituent Concentrations				
h (km)	T (°K)	M	ρ (gm cm^{-3})	P (dynes cm^{-2})	H (km)	n (cm^{-3})	n(N_2) (cm^{-3})	n(O_2) (cm^{-3})	n(N) (cm^{-3})	n(O) (cm^{-3})	n(He) (cm^{-3})	n(H) (cm^{-3})
100	206	28.04	9.50 (-10)*	5.91 (-1)	6.49	2.06 (13)	1.60 (13)	3.50 (12)	1.50 (9)	1.10 (12)	7.00 (7)	1.50 (5)
120	324	26.62	4.75 (-11)	4.80 (-2)	10.7	1.07 (12)	7.91 (11)	1.20 (11)	2.67 (8)	1.63 (11)	3.12 (7)	8.78 (4)
140	636	25.21	5.69 (-12)	1.19 (-2)	22.4	1.36 (11)	8.97 (10)	1.10 (10)	6.43 (7)	3.52 (10)	1.20 (7)	4.24 (4)
160	850	24.21	1.94 (-12)	5.67 (-3)	31.3	4.83 (10)	2.80 (10)	3.13 (9)	3.15 (7)	1.63 (10)	8.40 (6)	3.06 (4)
180	970	23.31	9.13 (-13)	3.16 (-3)	37.3	2.36 (10)	1.27 (10)	1.25 (9)	1.95 (7)	9.62 (9)	6.74 (6)	2.63 (4)
200	1060	22.47	4.80 (-13)	1.92 (-3)	42.6	1.31 (10)	6.31 (9)	5.60 (8)	1.32 (7)	6.21 (9)	5.06 (6)	2.36 (4)
250	1133	20.50	1.43 (-13)	6.56 (-4)	50.4	4.19 (9)	1.46 (9)	1.08 (8)	6.15 (6)	2.62 (9)	4.34 (6)	2.10 (4)
300	1157	19.05	5.10 (-14)	2.50 (-4)	56.5	1.61 (9)	3.62 (8)	2.34 (7)	3.11 (6)	1.20 (9)	3.32 (6)	1.96 (4)
350	1167	17.91	2.04 (-14)	1.10 (-4)	61.5	6.06 (8)	1.05 (8)	5.32 (6)	1.62 (6)	5.73 (8)	2.90 (6)	1.86 (4)
400	1175	17.11	8.83 (-15)	5.04 (-5)	65.8	3.11 (8)	2.96 (7)	1.26 (6)	8.50 (5)	2.77 (8)	2.41 (6)	1.76 (4)
500	1175	16.15	1.95 (-15)	1.18 (-5)	71.8	7.27 (7)	2.55 (6)	7.64 (4)	2.52 (5)	6.84 (7)	1.70 (6)	1.61 (4)
600	1175	15.38	4.85 (-16)	3.08 (-6)	77.6	1.90 (7)	2.36 (5)	5.03 (3)	7.65 (4)	1.75 (7)	1.21 (6)	1.48 (4)
700	1175	14.15	1.31 (-16)	9.05 (-7)	86.8	5.58 (6)	2.33 (4)	3.57 (2)	2.41 (4)	4.68 (6)	8.67 (5)	1.37 (4)
800	1175	12.02	3.87 (-17)	3.14 (-7)	105	1.94 (6)	2.46 (3)	2.73 (1)	7.84 (3)	1.29 (6)	6.29 (5)	1.28 (4)
900	1175	9.24	1.29 (-17)	1.37 (-7)	140	8.42 (5)	2.76 (2)	2.24 (0)	2.63 (3)	3.71 (5)	4.60 (5)	1.17 (4)
1,000	1175	6.80	5.19 (-18)	7.47 (-8)	196	4.60 (5)	3.29 (1)		9.05 (2)	1.10 (5)	3.40 (5)	1.06 (4)
1,200	1175	4.48	1.86 (-18)	3.40 (-8)	314	2.09 (5)			1.17 (2)	1.06 (4)	1.80 (5)	9.34 (3)
1,400	1175	3.91	7.67 (-19)	1.92 (-8)	379	1.18 (5)			1.66 (1)	1.16 (3)	1.00 (5)	8.13 (3)
1,600	1175	3.73	4.43 (-19)	1.16 (-8)	419	7.16 (4)			2.67 (0)	1.41 (2)	6.43 (4)	7.13 (3)
1,800	1175	3.50	2.70 (-19)	7.35 (-9)	457	4.53 (4)				1.91 (1)	3.90 (4)	6.20 (3)
2,000	1175	3.44	1.70 (-19)	4.83 (-9)	500	2.96 (4)				2.84 (0)	2.42 (4)	5.50 (3)
2,500	1175	2.97	6.07 (-20)	2.00 (-9)	651	1.23 (4)					8.00 (3)	4.24 (3)
3,000	1175	2.43	2.56 (-20)	1.03 (-9)	886	6.35 (3)					3.00 (3)	3.32 (3)
3,500	1175	1.96	1.28 (-20)	6.36 (-10)	1219	3.92 (3)					1.26 (3)	2.66 (3)
4,000	1175	1.62	7.30 (-21)	4.46 (-10)	1631	2.75 (3)					5.67 (2)	2.18 (3)
4,500	1175	1.39	4.85 (-21)	3.40 (-10)	2081	2.10 (3)					2.75 (2)	1.82 (3)
5,000	1175	1.25	3.51 (-21)	2.74 (-10)	2532	1.69 (3)					1.42 (2)	1.55 (3)
6,000	1175	1.11	2.22 (-21)	1.95 (-10)	3378	1.20 (3)					4.46 (1)	1.16 (3)
7,000	1175	1.05	1.61 (-21)	1.49 (-10)	4160	9.21 (2)					1.66 (1)	9.04 (2)
8,000	1175	1.03	1.26 (-21)	1.20 (-10)	4923	7.36 (2)					7.13 (0)	7.31 (2)
9,000	1175	1.02	1.03 (-21)	9.92 (-11)	5700	6.11 (2)					3.40 (0)	6.06 (2)
10,000	1175	1.01	8.70 (-22)	8.42 (-11)	6506	5.19 (2)					1.78 (0)	5.17 (2)

*Denotes $\rho = 9.50 \times 10^{-10}$ gm cm^{-3}

TABLE 8. Upper Atmosphere Neutral Properties vs. Altitude Near Sunspot Minimum

Altitude	Temp	Mol Wt.	Density	Pressure	Scale Ht.	Total Conc.	Constituent Concentrations					
h (km)	T (°K)	M	ρ (gm cm^{-3})	P (dynes cm^{-2})	H (km)	n (cm^{-3})	n(N_2) (cm^{-3})	n(O_2) (cm^{-3})	n(N) (cm^{-3})	n(O) (cm^{-3})	n(H_e) (cm^{-3})	n(H) (cm^{-3})
100	205	28.25	2.25(-10)*	1.35(-1)	6.35	4.80(12)	3.70(12)	9.00(11)	1.00(9)	2.00(11)	2.20(7)	5.00(5)
120	310	26.98	1.04(-11)	9.99(-3)	10.1	2.33(11)	1.74(11)	2.91(10)	1.77(8)	2.93(10)	9.98(6)	3.01(5)
140	560	25.74	1.36(-12)	2.47(-3)	19.3	3.19(10)	2.20(10)	2.96(9)	4.66(7)	6.94(9)	4.47(6)	1.58(5)
160	745	24.67	4.11(-13)	1.03(-3)	26.9	1.00(10)	6.28(9)	7.38(8)	2.16(7)	3.00(9)	2.93(6)	1.15(5)
180	860	23.68	1.75(-13)	5.28(-4)	32.6	4.45(9)	2.50(9)	2.63(8)	1.27(7)	1.67(9)	2.27(6)	9.67(4)
200	925	22.73	8.77(-14)	2.97(-4)	36.7	2.32(9)	1.16(9)	1.10(8)	8.33(6)	1.04(9)	1.91(6)	8.77(4)
250	990	20.55	2.17(-14)	8.68(-5)	44.1	6.35(8)	2.20(8)	1.67(7)	3.51(6)	3.93(6)	1.42(6)	7.74(4)
300	1000	18.78	6.74(-15)	2.99(-5)	49.5	2.16(8)	4.77(7)	2.91(6)	1.63(6)	1.63(8)	1.13(6)	7.26(4)
350	1000	17.50	2.39(-15)	1.14(-5)	53.9	8.24(7)	1.07(7)	5.28(5)	7.70(5)	6.94(7)	9.15(5)	6.88(4)
400	1000	16.61	9.28(-16)	4.64(-6)	57.7	3.36(7)	2.46(6)	9.93(4)	3.69(5)	2.99(7)	7.41(5)	6.52(4)
500	1000	15.20	1.65(-16)	9.04(-7)	64.9	6.55(6)	1.38(5)	3.66(3)	8.74(4)	5.77(6)	4.91(5)	5.89(4)
600	1000	13.03	3.42(-17)	2.13(-7)	77.9	1.58(6)	3.41(3)	1.49(2)	2.16(4)	1.77(6)	3.29(5)	5.33(4)
700	1000	9.50	8.28(-18)	7.24(-8)	110	5.25(5)	5.55(2)	6.69(0)	5.54(3)	2.47(5)	2.23(5)	4.84(4)
800	1000	6.13	2.58(-18)	3.49(-8)	175	2.53(5)	3.95(1)		1.48(3)	5.45(4)	1.53(5)	4.40(4)
900	1000	4.22	1.11(-18)	2.20(-8)	262	1.59(5)	3.02(0)		4.09(2)	1.26(4)	1.06(5)	4.01(4)
1,000	1000	3.36	6.36(-19)	1.57(-8)	338	1.14(5)			1.17(2)	3.01(3)	7.42(4)	3.67(4)
1,200	1000	2.68	3.05(-19)	9.46(-9)	447	6.85(4)			1.06(1)	1.93(2)	3.74(4)	3.09(4)
1,400	1000	2.28	1.73(-19)	6.32(-9)	553	4.58(4)			1.09(0)	1.43(1)	1.95(4)	2.63(4)
1,600	1000	1.95	1.07(-19)	4.56(-9)	679	3.30(4)				1.21(0)	1.06(4)	2.25(4)
1,800	1000	1.69	7.10(-20)	3.49(-9)	824	2.53(4)					8.84(3)	1.94(4)
2,000	1000	1.49	5.02(-20)	2.79(-9)	980	2.02(4)					3.23(3)	1.69(4)
2,500	1000	1.21	2.64(-20)	1.82(-9)	1350	1.32(4)					9.18(2)	1.22(4)
3,000	1000	1.09	1.72(-20)	1.31(-9)	1680	9.47(3)					2.90(2)	9.18(3)
3,500	1000	1.04	1.24(-20)	9.92(-10)	1951	7.19(3)					1.03(2)	7.09(3)
4,000	1000	1.02	9.58(-21)	7.80(-10)	2199	5.65(3)					4.04(1)	5.61(3)
4,500	1000	1.01	7.65(-21)	6.28(-10)	2440	4.35(3)					1.73(1)	4.34(3)
5,000	1000	1.01	6.26(-21)	5.17(-10)	2683	3.74(3)					7.97(0)	3.74(3)
6,000	1000	1.00	4.43(-21)	3.67(-10)	3188	2.66(3)					2.04(0)	2.66(3)
7,000	1000	1.00	3.31(-21)	2.75(-10)	3729	1.99(3)						1.99(3)
8,000	1000	1.00	2.58(-21)	2.14(-10)	4309	1.55(3)						1.55(3)
9,000	1000	1.00	2.07(-21)	1.72(-10)	4931	1.25(3)						1.25(3)
10,000	1000	1.00	1.71(-21)	1.42(-10)	5593	1.03(3)						1.03(3)

*Denotes 2.25×10^{-10} gm cm^{-3}

properties in order to derive the remainder. Usually the altitude variation of the mean molecular mass was introduced somewhat arbitrarily, thus a physically consistent vertical distribution of the composition could not be obtained. To avoid this approach, the model presented herein starts with density profiles from an empirical density model as primary input; the remaining properties are calculated using knowledge concerning the physics of the upper atmosphere together with boundary values derived from measurements.

This model cannot be described simply by a collection of equations, tables, and graphs. In order to provide the proper basis for understanding it, a description of the upper atmosphere is given first in Sections II and III in the form of a concise discussion summarizing the present knowledge of its composition and physics. Section IV explains the empirical density model used as a primary input for the property model in Section V. To illustrate the model, Section VI gives the results of computations made with an IBM-7090 in the form of two tables presenting the average atmospheric properties for sunspot maximum and minimum conditions, respectively. Also, these tables can be used to estimate the average atmospheric properties for the months immediately following the Argus (September 1958) and Starfish (July and August 1962) high-altitude nuclear detonations. Tables derived for many values of S' and t will be presented in a later report.

Flexibility has been stressed in the construction of the model in order to readily take advantage of new information as it becomes available. The model is developed mainly for the purpose of making predictions of atmospheric properties for comparison with measurements made from rockets and satellites.

Undoubtedly, the result of such comparisons will suggest changes in the model, hopefully tending toward an improved description of the atmosphere and more realistic model. Therefore, the model presented in this report must be considered the beginning of one attempt to achieve greater understanding of the upper atmosphere.

REFERENCES

Anderson, A. D., 1962, "A Simple Model for Atmospheric Density Variations from 200 to 800 km," J. Atmos. Sci., 19, 207-217.

_____, 1964, "On the Inexactness of the 10.7 cm Flux from the Sun as an Index of the Total Extreme Ultraviolet Radiation," J. Atmos. Sci., 21,1.

Beard, D. B., 1960, "The Interaction of the Terrestrial Field with the Solar Corpuscular Radiation," J. Geophys. Res., 65, 3559.

Bowles, K. L., 1962, "Profiles of Electron Density over the Magnetic Equator Obtained using the Incoherent Scatter Technique," U. S. National Bureau of Standards Report 7633, 1-6

Brandt, J. C., and J. W. Chamberlain, 1960, "Density of Neutral Gas in a Planetary Exosphere," Phys. Fluids, 3, 485-486.

Bourdeau, R. E., and S. J. Bauer, 1963, "Structure of the Upper Atmosphere Deduced from Charged Particle Measurements on Rockets and the Explorer VIII Satellite," Space Research III, New York, N.Y., Interscience Pub. Inc., 173-193.

Chapman, S., 1960, "Kinetic Theory of Gases: Viscosity, Thermal Conduction, and Diffusion," Fundamental Formulas of Physics, ed. D. H. Menzel, New York, N.Y., Dover, 290-306.

Court, A., A. J. Kantor, and A. E. Cole, 1962, "Supplemental Atmospheres," Air Force Cambridge Res. Lab. Res. Note 62-899, 20 pp.

Friedman, H., 1959, "Rocket Astronomy," J. Geophys. Res., 64, 1751.

Hanson, W. B., 1962, "Upper-Atmosphere Helium Ions," J. Geophys. Res., 67, 187.

Herring, J., and L. Kyle, 1961, "Density in a Planetary Exosphere, " J. Geophys. Res., 66, 1980-1982.

Hinteregger, H. E., 1962, "Absorption Spectrometric Analysis of the Upper Atmosphere in the EUV Region," J. Atmos. Sci., 19, 351.

Johnson, F. S., 1956, "Temperature Distribution of the Ionosphere under Control of Thermal Conductivity," J. Geophys. Res., 61, 71-76.

_____, 1958, "Temperatures in the High Atmosphere," Annales de Geophysique, 14, 94-108.

_____, 1960b, "The Ion Distribution above the F_2 Maximum," J. Geophys. Res., 65, 577-584.

_____, 1961a, Satellite Environment Handbook, Stanford, Calif., Stanford Univ. Press, 17.

_____, 1961b, "The Distribution of Hydrogen in the Telluric Hydrogen Corona," Astrophys. J., 133, 701-705.

Kallmann, H. K., 1959, "A Preliminary Model Atmosphere Based on Rocket and Satellite Data," J. Geophys. Res., 64, 620.

Kupperian, J. E., et al., 1960, "Molecular Oxygen Densities in the Mesophere over Ft. Churchill," Ann. Intern. Geophys. Yr., 12, part 1, 440-444.

Mange, P., 1960, "The Distribution of Minor Ions in Electrostatic Equilibrium in the High Atmosphere," J. Geophys. Res., 65, 3833-3834.

Meadows, E. B., and J. W. Townsend, 1960, "IGY Rocket Measurements of Arctic Composition above 100 km," Space Research, New York, N.Y., Interscience Pub. Inc., 175-198.

Nicolet, M., 1959, "The Constitution and Composition of the Upper Atmosphere," Proc. Inst. Radio Eng., 47, 142-146.

_____, 1960, "The Properties and Constitution of the Upper Atmosphere," Physics of the Upper Atmosphere, ed. J. Ratcliffe, New York, N.Y., Academic Press, Chp. 2.

_____, 1961, "Helium, an Important Constituent in the Lower Exosphere," J. Geophys. Res., 66, 2263-2264.

Opik, E. J., and S. F. Singer, 1960, "Distribution of Density in a Planetary Atmosphere," Phys. Fluids, 3, 486-488.

Pokhunkov, A. A., 1962, "Gravitational Separation, Composition and Structural Parameters of the Atmosphere at Altitudes above 100 km," Space Research III, New York, N.Y., Interscience Pub. Inc., 132.

Schaefer, E. J. 1963, "The Dissociation of Oxygen Measured by a Rocket-Borne Mass Spectrometer," J. Geophys. Res., 68, 1175-1176.

_____, and M. H. Nichols, 1961, "Mass Spectrometer for an Upper Air Measurement," ARS J., 31, 1773.

_____, 1963, "Recent Results from a Rocket-Borne Mass Spectrometer," Space Research IV, New York, N.Y., Interscience Pub. Inc., to be published.

Sharp, G. W., 1962, "The Concept of Temperature in the Upper Atmosphere," Temperature - Its Measurement and Control in Science and Industry, 3, part I, New York, N.Y., Reinhold Pub. Corp., 823-829.

Spitzer, L., 1949, "The Terrestrial Atmosphere above 300 km," Atmospheres of the Earth and Planets, ed. G. P. Kuiper, Chicago, Illinois, Univ. Chicago Press, chp. 7.

_____, 1952, "Ideal Plasma," Astrophys. J., 116, 299.

U. S. Standard Atmosphere, 1962, 1962, Washington, D.C., U.S. Govt.Print.Off., 278 pp.

Appendix A

THE NEUTRAL DISTRIBUTION OF DENSITY IN A MODEL EXOSPHERE

William E. Francis

Appendix A

THE NEUTRAL DISTRIBUTION OF DENSITY IN A MODEL EXOSPHERE

Several authors have considered the problem of extending the vertical hydrostatic distribution of neutrals beyond the base of the exosphere where collisions are so infrequent that the barometric law is no longer strictly applicable (Brandt and Chamberlain, 1960; Johnson and Fish, 1960; Johnson, 1961, and Opik and Singer, 1959, 1961). Spherical symmetry is assumed by each author and collisions above the base of the exosphere are ignored. Both Opik and Singer (1961) and Johnson (1961) classify the exospheric particles as to orbital type and give equations in the form of definite integrals over velocity space that describe their distribution. Their numerical results (obtained by numerical integration) appear to be consistent.

Johnson divides the Maxwellian velocity distribution of exospheric particles into four groups depending on their trajectories with reference to the base of the exosphere. These four types are: (1) ballistic elliptic, (2) orbital elliptic, (3) ballistic hyperbolic, and (4) orbital hyperbolic. The corresponding normalized groups are designated x_1, x_2, x_3, and x_4 respectively. The author has found that it is not too difficult to express these fractional groups in terms of error functions and thus eliminate the need for numerical integration. It is the purpose of this note to illustrate the analytic expressions for the above distributions and to show that quite

simple expressions can be used to approximate exospheric densities out to about 5 earth radii. It is hoped that such a contribution will simplify the use of the results of previous authors.

It has been argued that exospheric particles in group χ_4 and particles incident on the earth in group χ_3 do not exist. One must therefore eliminate the fraction $\chi_4 + 1/2\ \chi_3$ of particles in the hydrostatic distribution since they are not present in the real distribution. However, there is some disagreement as to whether particles in the trapped orbits corresponding to group χ_2 are present or not. Brandt and Chamberlain (1960) argue that these orbits are populated, while Opik and Singer (1960) argue they are not. Johnson (1961) suggests that trapped orbits are probably populated out to 6 or 7 earth radii but that at greater distances a transition occurs to a region free of trapped particles.

The analytic expressions for the orbital types corresponding to the definite integrals given by Johnson are:

$$\chi_1 = \mathrm{erf}\,(\alpha V_e) - \sqrt{4/\pi}\,(\alpha V_e)\exp(-\alpha^2 V_e^{\,2}) - \sqrt{1-(r_o/r)^2}\left\{\mathrm{erf}\,(\alpha V_o\sqrt{r/r_o}) - \sqrt{4/\pi}(\alpha V_o\sqrt{r/r_o})\exp(-\alpha^2 V_o^{\,2} r/r_o)\right\}\exp(-\alpha^2 V_o^{\,2}), \qquad (1)$$

$$\chi_2 = \sqrt{1-(r_o/r)^2}\left\{\mathrm{erf}\,(\alpha V_o\sqrt{r/r_o}) - \sqrt{4/\pi}\,(\alpha V_o\sqrt{r/r_o})\exp(-\alpha^2 V_o^{\,2} r/r_o)\right\}\exp(-\alpha^2 V_o^{\,2}), \qquad (2)$$

$$\chi_3 = 1 - \mathrm{erf}\,(\alpha V_e) + \sqrt{4/\pi}\,(\alpha V_e\exp(-\alpha^2 V_e^{\,2}) -$$

$$\sqrt{1 - (r_o/r)}^2 \left\{ 1 - \mathrm{erf}\,(\alpha V_o \sqrt{r/r_o}) + \right.$$

$$\left. \sqrt{4/\pi}\,(\alpha V_o \sqrt{r/r_o}) \exp\,(-\alpha^2 V_o{}^2 r/r_o) \right\} \exp\,(-\alpha^2 V_o{}^2), \qquad (3)$$

$$x_4 = \sqrt{1 - (r_o/r)}^2 \left\{ 1 - \mathrm{erf}\,(\alpha V_o \sqrt{r/r_o}) + \right.$$

$$\left. \sqrt{4/\pi}\,(\alpha V_o \sqrt{r/r_o}) \exp\,(-\alpha^2 V_o{}^2 r/r_o) \right\} \exp\,(-\alpha^2 V_o{}^2) \qquad (4)$$

where

$$\alpha^2 = m/2kT,$$

$$V_e{}^2 = 2ga^2/r,$$

$$V_o{}^2 = r_o V_e{}^2/(r + r_o),$$

$$\mathrm{erf}\,(Z) = \sqrt{4/\pi} \int_0^Z \exp\,(-t^2)dt,$$

r is the distance from the earth's center, r_o is the distance from the center of the earth to the base of the exosphere, a is the radius of the earth, g is the acceleration of gravity at the earth's surface, m is the mass of the particle, T is the temperature, and k is the Boltzmann constant. The above expressions can also be expressed in terms of the scale height H, since $\alpha^2 V_e{}^2 = r/H$.

The following combinations are also useful:

$$x_1 + x_2 = \mathrm{erf}\,(\alpha V_e) - \sqrt{4/\pi}\,(\alpha V_e) \exp\,(-\alpha^2 V_e{}^2), \qquad (5)$$

$$x_3 + x_4 = 1 - \mathrm{erf}\,(\alpha V_e) + \sqrt{4/\pi}\,(\alpha V_e) \exp\,(-\alpha^2 V_e{}^2), \qquad (6)$$

$$x_2 + x_4 = \sqrt{1 - (r_o/r)^2} \exp(-\alpha^2 V_o^2), \tag{7}$$

and

$$x_1 + x_3 = 1 - \sqrt{1 - (r_o/r)^2} \exp(-\alpha^2 V_o^2) . \tag{8}$$

As one might expect, $x_1 + x_2$ and $x_3 + x_4$ are independent of r_o since these two groups comprise the total fraction of particles with velocities less than escape velocity and greater than escape velocity respectively, and this property is clearly independent of a reference sphere. The purpose of a reference sphere is to permit distinction between orbital and ballistic particles. It is interesting to note that the use of a reference sphere introduces a discontinuity at the base of the exosphere since from (3) $1/2\ X_3(r_o) > 0$. However, this discontinuity is very small and indicates that ignoring collisions above this somewhat arbitrary sphere is a very good approximation. The above expressions are very slowly varying functions of r_o.

With trapped orbits fully populated, the fraction $x_1 + x_2 + 1/2\ x_3$ of the hydrostatic distribution represents the actual distribution. The fraction $x_1 + 1/2\ x_3$ of the hydrostatic distribution represents the ballistic distribution (trapped orbits absent). It can be readily seen from Eqs. (1), (2) and (3) that the analytic expressions for the fractions $x_1 + x_2 + 1/2\ x_3$ and $x_1 + 1/2\ x_3$ are somewhat unwieldy. Herring and Kyle (1961) and Aamodt and Case (1962) have previously given the lengthy analytic expressions for the special case of a ballistic density distribution in terms of error

functions. However, it turns out that χ_3 is much smaller than χ_1 below about 5 earth radii. Therefore, below this altitude it is permissible to neglect 1/2 χ_3 and to use the much simpler expression (5) and (8) to correct the hydrostatic distribution.

The hydrostatic density distribution is given by

$$\rho(r) = \rho(r_o) \exp \left\{ \alpha^2 V_e^2 (1 - r/r_o) \right\} . \tag{9}$$

We have then approximately

$$\rho_b(r) \cong \left\{ 1 - \sqrt{1 - (r_o/r)^2} \exp(-\alpha^2 V_o^2) \right\} \rho(r) \tag{10}$$

and

$$\rho_t(r) \cong \left\{ \mathrm{erf}(\alpha V_e) - \sqrt{4/\pi}(\alpha V_e) \exp(-\alpha^2 V_e^2) \right\} \rho(r) \tag{11}$$

where $\rho_b(r)$ is the density assuming only ballistic orbits are present and $\rho_t(r)$ is the density with the trapped orbits fully populated ($\rho_t > \rho_b$). The overestimate in using (10) and the underestimate in using (11) amounts to only about 10% and 4% respectively at a distance of 5 earth radii from the center of the earth and with an isothermal temperature of 1250 K. The error increases slowly with increasing temperature and distance from the earth. It is not too difficult to justify the use of (10) and (11) since (a) they are very good approximations below 5 earth radii, (b) it is unlikely

that the trapped orbits are either completely populated or completely unpopulated (the above approximations give results that lie between ρ_t and ρ_b), and (c) the expressions (1), (2), (3) and (4) are only approximations based on a simplified model.

REFERENCES (Appendix A)

Aamodt, R. E., and K. M. Case, 1962, "Density in a Simple Model of the Exosphere," Phys. Fluids, 5, 1019-1021.

Brandt, J. C., and J. W. Chamberlain, 1960, "Density of Neutral Gas in a Planetary Exosphere," Phys. Fluids, 3, 485-486.

Herring, J., and L. Kyle, 1961, "Density in a Planetary Exosphere," J. Geophys. Res., 66, 1980-1982.

Johnson, F. S., and R. A. Fish, 1960, "The Telluric Hydrogen Corona," Astrophys. J., 131, 502-515.

Johnson, F. S., 1961, "The Distribution of Hydrogen in the Telluric Hydrogen Corona," Astrophys. J., 133, 701-705.

Opik, E. J., and S. F. Singer, 1959, "Distribution of Density in a Planetary Exosphere," Phys. Fluids, 2, 653-655.

Opik, E. J., and S. F. Singer, 1960, "Distribution of Density in a Planetary Exosphere," Phys. Fluids, 3, 486-488.

Opik, E. J., and S. F. Singer, 1961, "Distribution of Density in a Planetary Exosphere: II," Phys. Fluids, 4, 221-233.

LIST OF LEGENDS FOR FIGURES

Fig. 1. Distribution of atomic hydrogen vs. altitude above the earth at the extremes of the sunspot cycle (Johnson, 1961a). The curve labeled 1500 K is for the average temperature corresponding to the maximum of the sunspot cycle, while the curve labeled 1000 K corresponds to the sunspot minimum.

Fig. 2. Fraction of Maxwellian particles in the atmosphere vs. altitude for three temperatures and two cases.

Fig. 3. Penetration of solar radiation into the atmosphere according to Friedman (1959). The graph shows the altitude at which a fraction e^{-1} remains of the radiation incident on the atmosphere.

Fig. 4. Isothermal temperature (above 400 km) vs. S' for every hour.

Fig. 5. Electron concentrations vs. geopotential altitude for temperatures of 750 K and 1300 K, respectively (Bowles, 1962).

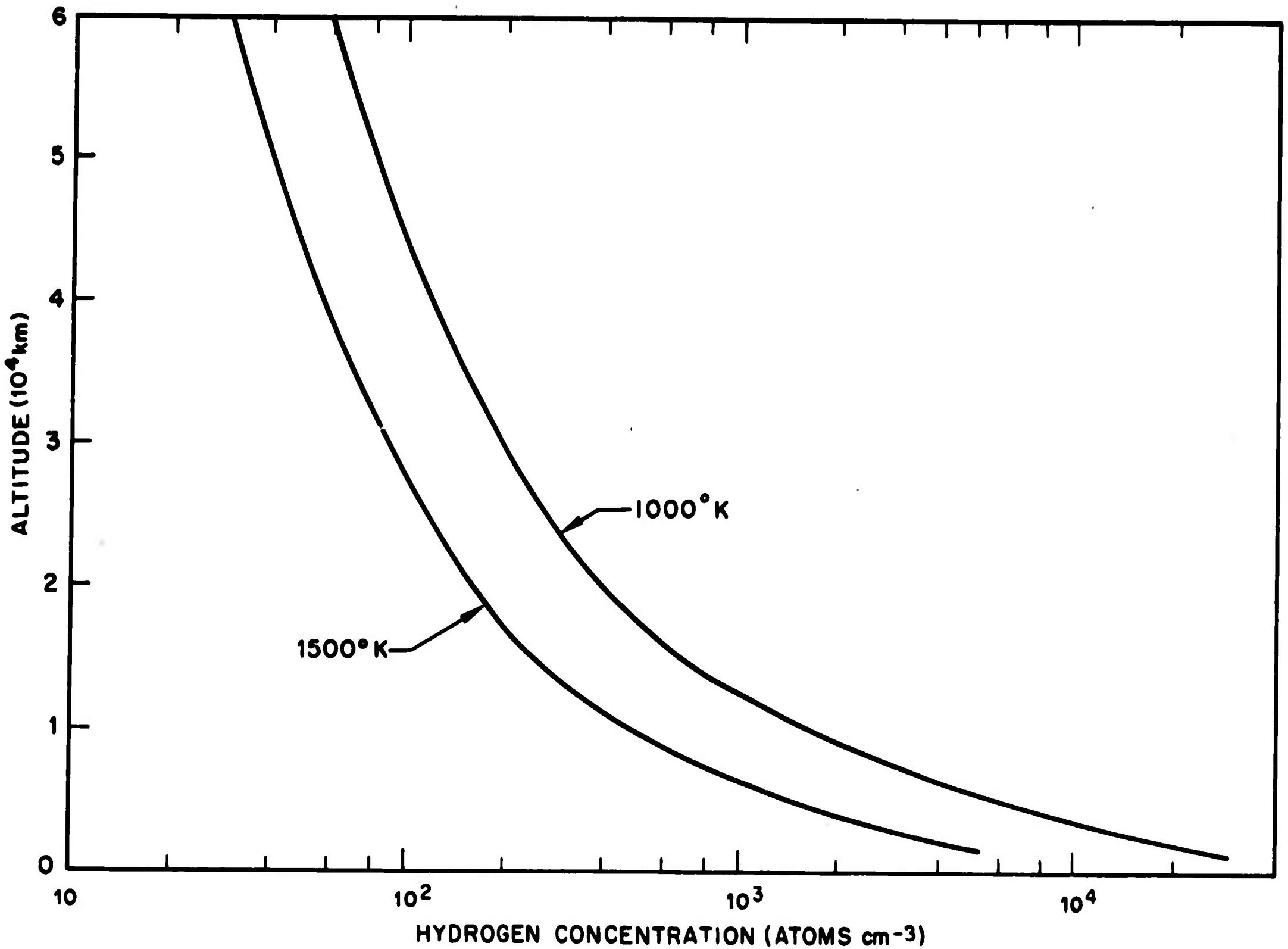
6
5
4
3
2
1
0
ALTITUDE (10^4 km)
1000°K
1500°K
10
10^2
10^3
10^4
HYDROGEN CONCENTRATION (ATOMS cm^{-3})

Figure 1

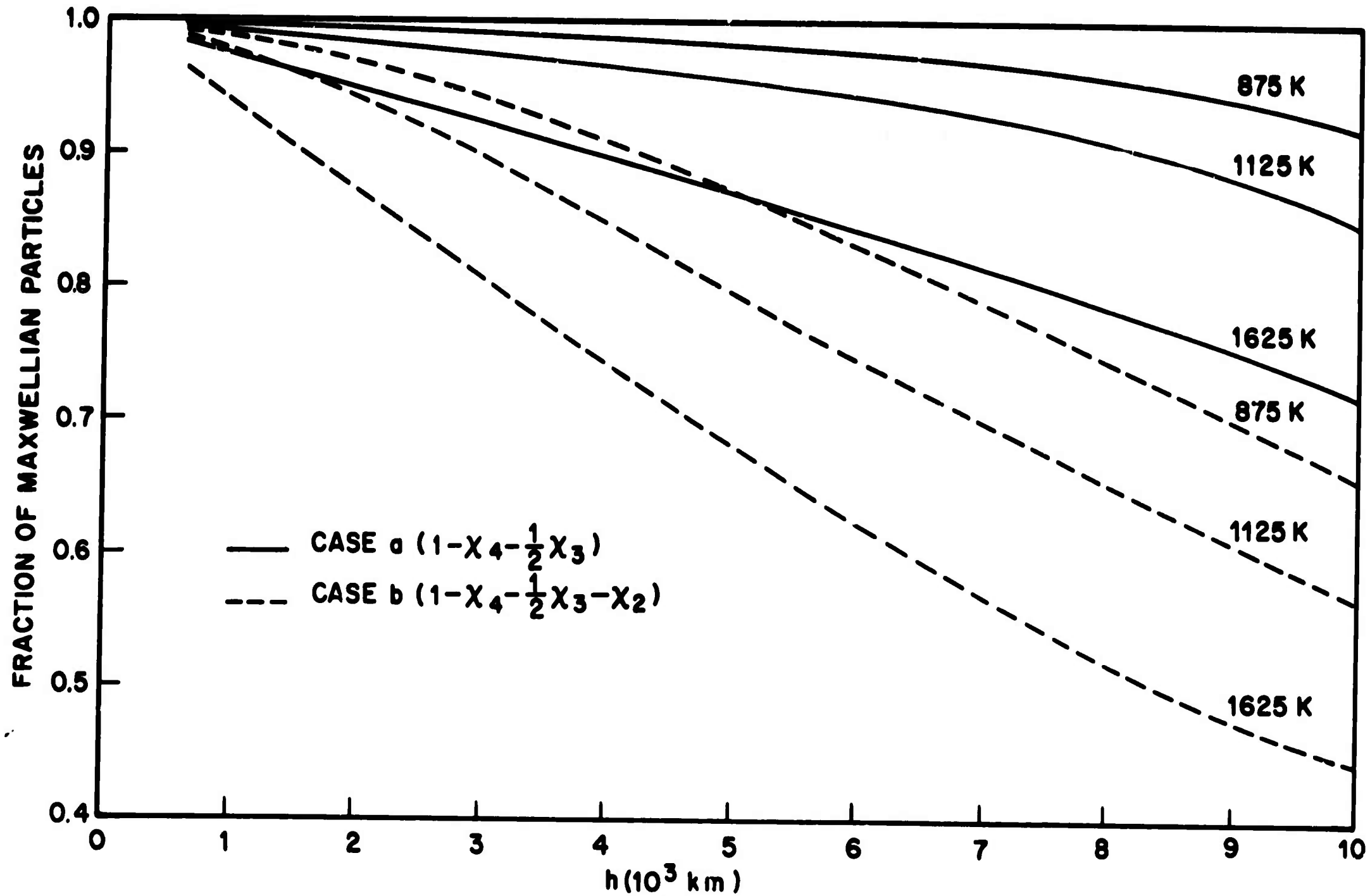
1.0
0.9
0.8
0.7
0.6
0.5
0.4
FRACTION OF MAXWELLIAN PARTICLES
0
1
2
3
4
5
6
7
8
9
10
h(10³ km)
875 K
1125 K
1625 K
875 K
1125 K
1625 K
CASE a (1-X4-½X3)
CASE b (1-X4-½X3-X2)

Figure 2

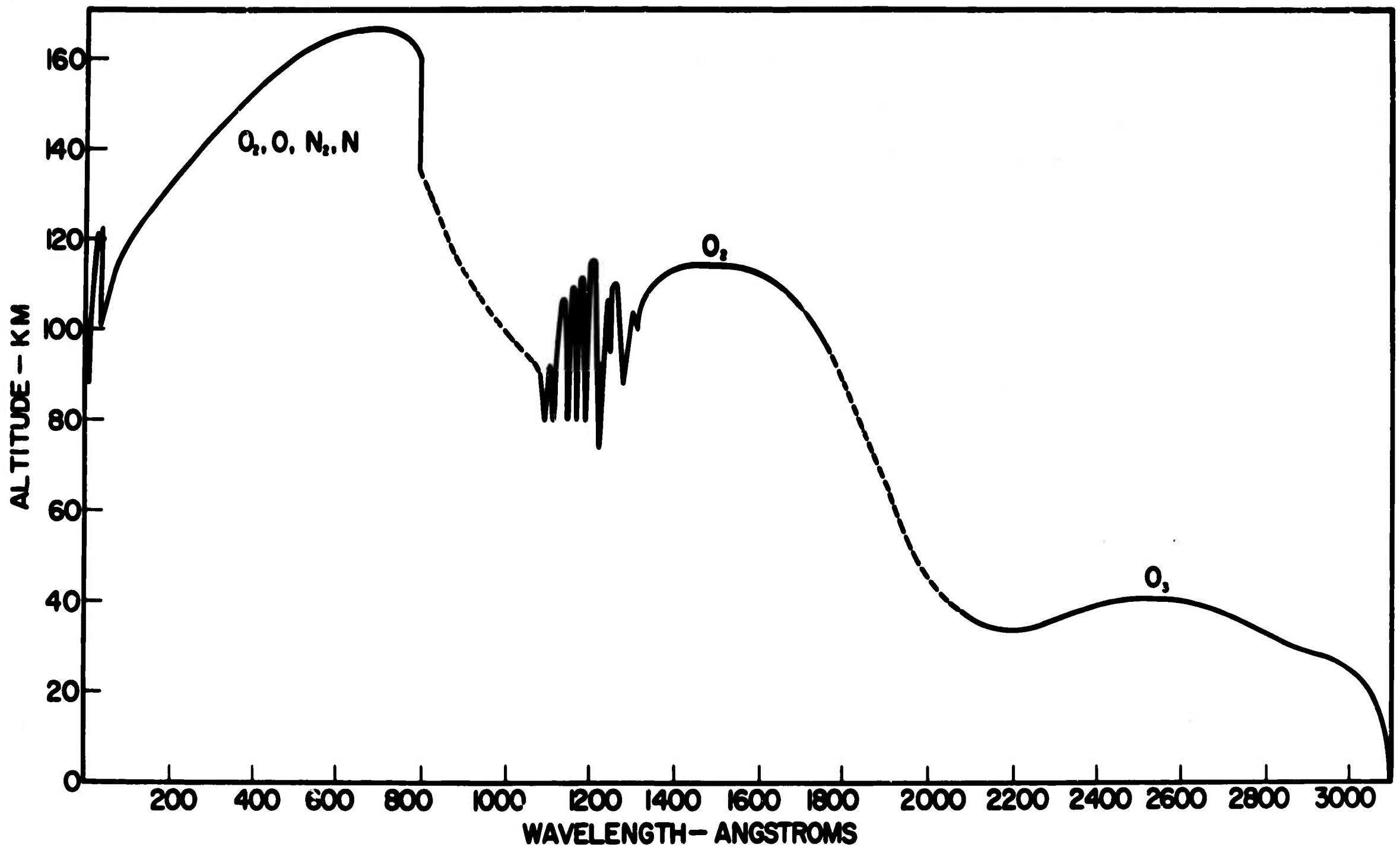

Figure 3

Fig. 3

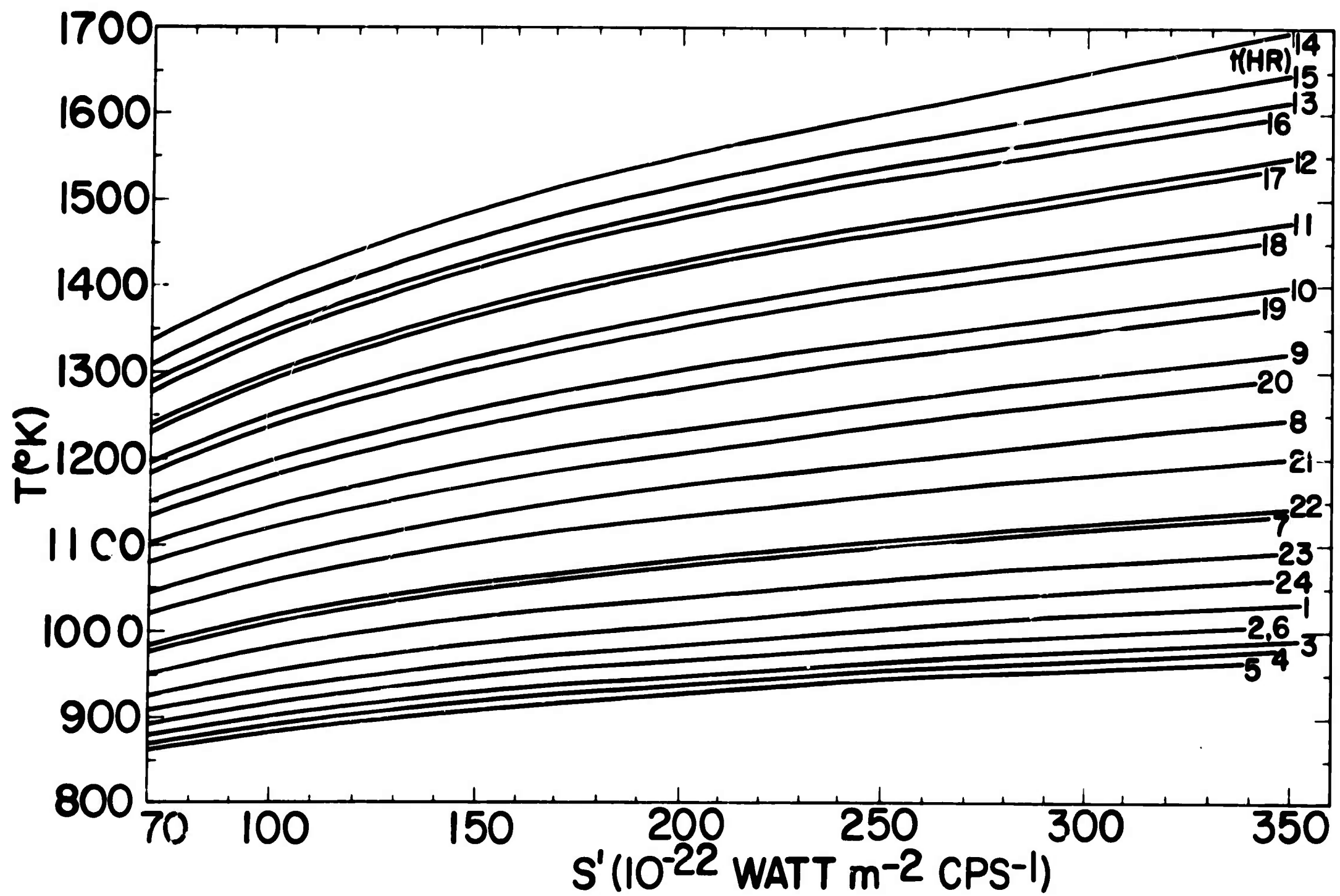
1700
1600
1500
1400
1300
1200
1100
1000
900
800
T(°K)
70
100
150
200
250
300
350
S' (10^-22 WATT m^-2 CPS^-1)
τ(HR)
14
15
13
16
12
17
11
18
10
19
9
20
8
21
22
7
23
24
1
2,6
3
4
5

Figure 4

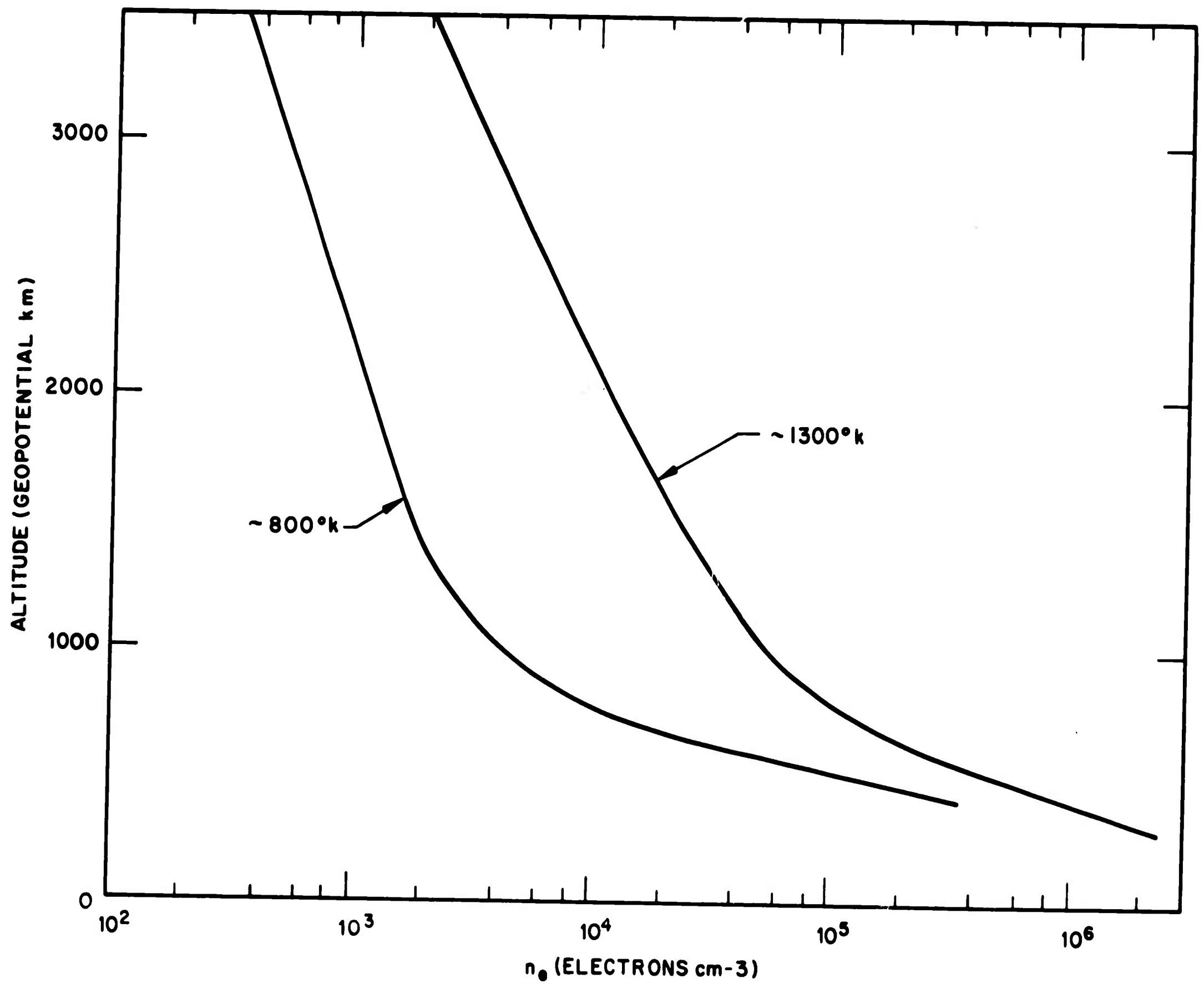
3000
2000
1000
0
ALTITUDE (GEOPOTENTIAL km)
~1300°k
~800°k
10^2
10^3
10^4
10^5
10^6
n_e (ELECTRONS cm-3)

Figure 5